Elaboration, by tape casting, of an SOFC half cell for low temperature applications

Claire Bonhomme, S. Beaudet-Savignat, A.L. Sauvet, Bernard Soulestin, Thierry Chartier

J.G.Heinrich and C. Aneziris, Proc. 10th ECerS Conf., Göller Verlag, Baden-Baden, 2007, 885-889, ISBN: 3-87264-022-4

Elaboration, by tape casting, of an SOFC half-cell for low temperature applications

Claire Bonhomme* [1,2], Sophie Beaudet-Savignat[2], Anne-Laure Sauvet[2], Bernard Soulestin[1], Thierry Chartier[1]

[1] Laboratoire Sciences des Procédés Céramiques et Traitements de Surface, SPCTS, CNRS, 47 Avenue Albert Thomas 87065 LIMOGES, France.

[2]. Laboratoire de Céramiques et Composants Avancés, CEA Le Ripault, BP 16 37260 MONTS, France.

Abstract

These last past years, a major interest has been devoted to decrease the working temperature of solid oxide fuel cells (SOFCs) down to about 700°C. In this respect, materials with a high ionic conductivity at low temperature have to be found and the process to elaborate fuel cells, using these new materials, has to be developed.

Apatite materials ($La_{10-x}Sr_x(SiO_4)_6O_{3-x/2}$) are attractive candidates for solid electrolytes. The apatite powder (x = 1) with a 0.75 µm mean particle size, produced by solid state reaction, was tape cast to obtain green sheets with a thickness of about 260 µm. After sintering at 1400°C-2h, the relative density of the electrolyte was 98.2%. No secondary phase was detected by X ray diffraction. The ionic conductivity of the apatite is equal to 2.5 10^{-3} S/cm at 700°C. It has been shown that this conductivity doesn't increase with the grain size of the material when the apatite is sintered at 1400°C for different dwell times. However, a jump in the ionic conductivity is observed when the material is sintered at 1500°C.

Concerning the cathode, perovskite oxides ($La_{1-x}Sr_xMn_{1-y}Co_yO_{3-\delta}$) have been chosen. The perovskite powder with a 2.8 µm mean particle size was also shaped by tape casting. The required porosity in the sintered cathode was obtained by introducing a pore forming agent (corn starch) in the tape casting slurry.

The symmetrical cell cathode/electrolyte/cathode was fabricated by stacking layers obtained by tape casting and co-sintering at 1400°C for 2 h in air. Impedance spectroscopy measurements were performed on this cell in order to determine the electrode resistance.

Introduction

Lowering the working temperature of a SOFC system down to 700°C has a great importance to reduce thermal stresses, to decrease the cost of the system and to improve the lifetime of the system. In this respect, the development of new electrolyte and electrode materials with high ionic conductivities at 700°C is required.

One candidate for the electrolyte material is a ceramic with apatite structure: $La_9Sr_1Si_6O_{26.5}$. This material has attracted considerable attention because of its high ionic conductivity at 700°C and its chemical stability for a pO_2 varying from 10^{-25} to 0.21 [1-9]. Brisse et al [10] have shown that the electronic transport number of the apatite material $La_9Sr_1Si_6O_{26.5}$ is close to 0, indicating that this material is a pure ionic conductor. The structure consists of isolated and covalent silicate tetrahedra (SiO_4) which form the rigid part of the structure. The La_6 cations are located in a seven coordinated site (named 6h) and form a tunnel along the "c" axis. The La_4 cations are located in a nine coordinate site named 4f. The oxygen anions are located in the tunnel formed by the La_6 cations and are responsible for the ionic conductivity of this material [11].

The cathode material is a perovskite oxide $La_{0.75}Sr_{0.25}Mn_{0.8}Co_{0.2}O_{3-\delta}$ which exhibit mixed ionic and electronic conducting properties and a relatively low thermal expansion coefficient [12]. The cathode should have an open porosity of 30% for efficient gas transportation and its chemical reactivity with apatite material must be avoided.

Symmetrical cathode/electrolyte/cathode half cells have been fabricated by tape casting of suspensions of $La_9Sr_1(SiO_4)_6O_{2.5}$ electrolyte and $La_{0.75}Sr_{0.25}Mn_{0.8}Co_{0.2}O_{3-\delta}$ cathode powders, lamination, debinding and co-sintering. The dilatometric behaviors, during sintering, of the two materials have been controlled and adapted by means of the powder and suspensions characteristics, in order to prevent cracks, delaminations or deformations during co sintering. The thermal expansion coefficients of the electrolyte and cathode materials are closely matched, that is necessary to minimise stresses in the co-sintered half-cell.

Experimental procedure

The $La_9Sr_1(SiO_4)_6O_{2.5}$ powder was synthesized using a solid state reaction. Ultra pure oxides and carbonates precursors, i.e. La_2O_3 (99.99%, Ampère Industrie, France), SiO_2 (99.99%, Cerac, France) and $SrCO_3$ (99.99%, Alfa Aesar, France) were used. The mixture was attrition-milled using 0.8 mm-diameter zirconia balls in water for 3h30 and dried. The synthesis temperature to form the apatite structure is 1400°C. Then, the synthesized powder was attrition-milled in alcohol using a dispersant (phosphate ester, 1 wt% on the powder base). Attrition-milling was stopped when the particle size reached a monomodal distribution

with a mean particle size of 0.75 µm (laser granulometer - Mastersizer 2000, Malvern Instruments). Finally, the suspension was dried.

The $La_{0.75}Sr_{0.25}Mn_{0.8}Co_{0.2}O_{3-\delta}$ powder was provided by Praxair, USA. The perovskite powder was calcined at 1150°C for 2 hours in order to adapt its reactivity to the apatite powder. After calcination, the perovskite powder has a bimodal particle size distribution with a mean particle size of 2.8 µm.

The gas-tight $La_9Sr_1(SiO_4)_6O_{2.5}$ apatite ceramic and the porous layers of $La_{0.75}Sr_{0.25}Mn_{0.8}Co_{0.2}O_{3-\delta}$ perovskite were elaborated by tape casting. The porous structure of the cathode was obtained by introducing a pore forming agent (PFA) in the perovskite tape casting suspension. Fourteen micrometers mean diameter corn-starch particles were used as PFA because of their narrow particle size distribution and their total combustion during the thermal treatment. PFA volume fractions of 40.2 and 42.2% were used in order to obtain an interconnected porosity. The green tape thickness was 260 µm for the electrolyte and 95 µm for the cathode. Thirty millimeter-diameter disks were then punched in the green tapes. Identical layers were stacked to obtain dense monolithic electrolyte and cathode materials for characterization. The symmetrical cell cathode/electrolyte/cathode was elaborated by stacking five electrolyte layers and one cathode layer on each side of the electrolyte. The stacks were then laminated under 40 MPa at 85°C. The organics introduced in the tape casting suspensions were burn out by slow heating rate (0.3°C/min) in air up to 600°C. Co-sintering of the symmetrical cathode/electrolyte/cathode half-cell was performed in air during 2h at 1400°C with a 5°C/min heating rate.

In order to evaluate the influence of the grain size on the ionic conductivity, the electrolyte material was sintered at 1400°C for 2, 6 and 10h and at 1500°C for 8h.

The densities of these materials were measured using the Archimedes method. Microstructures were observed by SEM (S-2500, Hitashi) on polished cross sections after a thermal etching of grain boundaries. The SEM micrographs were analyzed using an image analyzer (Aphelion software). Grain size distributions and grain boundary densities of the sintered electrolyte material were evaluated on at least 1000 grains for each sintering condition.

Transmission Electron Microscopy (TEM), combined with Energy Dispersive X-ray Spectrometry (EDS), was performed on the 1400°C-2h and 1500°C-8h sintered electrolyte materials in order to verify the purity of the grain boundaries.

The eventual interface reactions between $La_9Sr_1(SiO_4)_6O_{2.5}$ and $La_{0.75}Sr_{0.25}Mn_{0.8}Co_{0.2}O_{3-\delta}$, after co-sintering, was investigated by SEM on fractured sections, combined with EDS.

Electrochemical measurements were carried out on samples of $La_9Sr_1(SiO_4)_6O_{2.5}$ and on symmetrical cell cathode/electrolyte/cathode using AC impedance spectroscopy. Pt mesh was used as current collectors. The measurements were performed in air between 300 and 800 °C, with a 30 mV signal amplitude at open circuit voltage in the 10^6-10^{-3} Hz frequency range. Nyquist diagrams obtained were fitted using Zview software [13].

Results and discussion

Electrolyte material

The optimum sintering conditions of the electrolyte material, leading to nearly full density (98.7%), were found to be 1400°C with a 2h dwell time. An increase of the dwell time at 1400°C or an increase of the sintering temperature at 1500°C leads to grain growth without loss of density (fig. 1 and table 1).

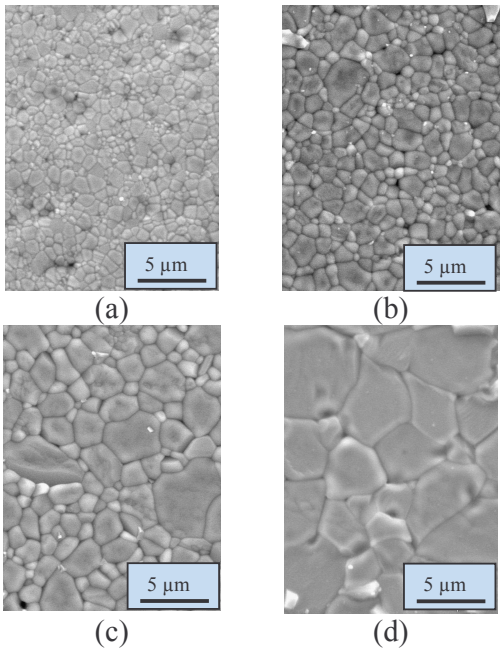

Fig.1. SEM micrographs of $La_9Sr_1(SiO_4)_6O_{2.5}$ electrolyte material sintered in air at 1400°C for 2h (a), 6h (b), 10h (c) and at 1500°C for 8h (d).

Sintering conditions	Relative density (%)	Mean grain size (µm)	Grain boundary density (µm/µm^2)
1400°C-2h	98.2	0.68	3.98
1400°C-6h	99	0.79	3.24
1400°C-10h	99.4	1.5	1.57
1500°C-8h	99.4	3.9	0.61

Table.1. Influence of sintering conditions on the microstructure of apatite material.

The conductivity of apatite materials $La_9Sr_1(SiO_4)_6O_{2.5}$ sintered at 1400 and 1500°C, as well as the undoped compound $La_{9.33}(SiO_4)_6O_2$, was measured by impedance spectroscopy (fig.2 and table 2).

First, we notice the low conductivity for the undoped apatite and the significant increase when the La-site is doped with Sr. The activation energy for $La_{9.33}(SiO_4)_6O_2$ (0.89 eV) is higher than for $La_9Sr_1(SiO_4)_6O_{2.5}$ (0.79 eV).
The ionic conductivity of the $La_9Sr_1(SiO_4)_6O_{2.5}$ apatite compound doesn't change with the dwell time at 1400°C, although the mean grain size of this material is increasing by a factor of 2 : 0.68µm for a 2h and 1.5µm for a 10h dwell-time (table 1). However, a jump in the ionic conductivity is observed when the apatite is sintered at 1500°C for 8h (d_{50}=3.9 µm).

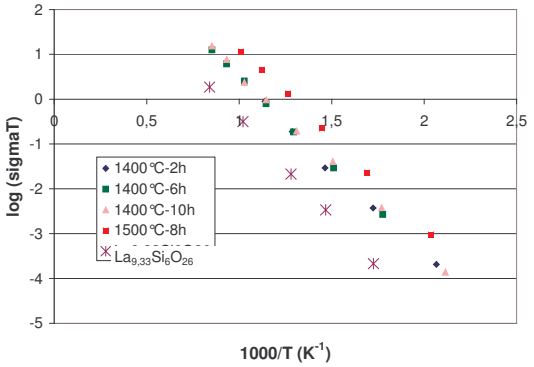

Fig.2. Arrhenius plots of the undoped apatite $La_{9.33}(SiO_4)_6O_2$ and of $La_9Sr_1(SiO_4)_6O_{2.5}$ apatite sintered at 1400°C for 2, 6 and 10h and at 1500°C for 8h.

Sintering conditions	Ionic conductivity at 700°C (S/cm)	Activation energy (eV)
1400°C-2h	$2.5\ 10^{-3}$	0.78
1400°C-6h	$2.6\ 10^{-3}$	0.79
1400°C-10h	$2.4\ 10^{-3}$	0.78
1500°C-8h	$1.2\ 10^{-2}$	0.793
$La_{9.33}Si_6O_{26}$	$3\ 10^{-4}$	0.89

Table 2. Ionic conductivity and activation energy values for the $La_9Sr_1(SiO_4)_6O_{2.5}$ apatite sintered at 1400°C and 1500°C, compared to the undoped apatite $La_{9.33}Si_6O_{26}$.

For a better understanding of the conductivity evolution of the apatite material, TEM was performed on the $La_9Sr_1(SiO_4)_6O_{2.5}$ apatite sintered at 1400°C for 2h and 1500°C for 8h (fig.3) in order to detect eventual secondary phases, mainly located at grain boundary.

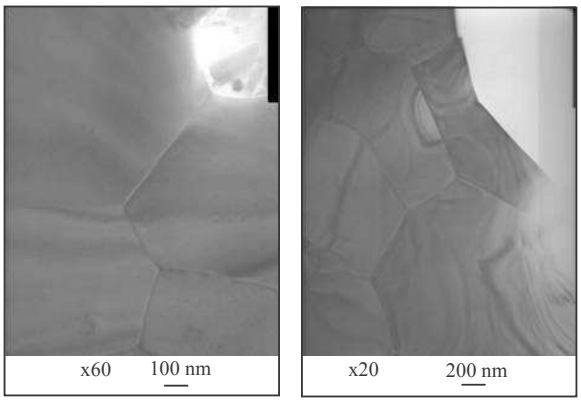

(a) (b)

Fig.3. TEM images of the $La_9Sr_1(SiO_4)_6O_{2.5}$ apatite material sintered at (a) 1400°C-2h and (b) 1500°C-8h.

The grain boundaries are secondary phase free for the two sintering conditions. However, white crystals are observed when the apatite is sintered at 1400°C-2h. They correspond to La_2SiO_5 or $La_2Si_2O_7$ phases according to EDS analysis. These insulating secondary phases reduce the ionic conductivity of the apatite material. In addition, the presence of these phase modify the stoechiometry of surrounding apatite material. The absence of secondary phases and the low value of grain boundary density (table 1) in the apatite sintered at 1500°C-8h could be an explanation of the jump in ionic conductivity.
TEM observation of the apatite sintered at 1400°C for 10h is under way in order to verify the presence of secondary phases, which could explain the non evolution of the ionic conductivity at 1400°C whereas grain growth was observed with the dwell-time.

Symmetrical cell cathode/electrolyte/cathode

Porous cathodes with porosity of 34.8% and 35.8% were elaborated by tape casting and sintered in air at 1400°C-2h.
The conductivity, at 700°C, is larger for the less porous cathode (table 3).

	PFA volume fraction (%)	Porosity (%)	Conductivity at 700°C (S/cm)
Cathode 1	42.2	35.8	0.092
Cathode 2	40.2	34.8	0.126

Table.3. Conductivity of cathode materials for two porosities.

Symmetrical cells, cathode/electrolyte/cathode, with cathode of two porosities, were co-sintered in air at 1400°C-2h (fig.4). The thickness is about 560µm for the dense electrolyte and 60µm for the ex-corn starch porous cathodes.

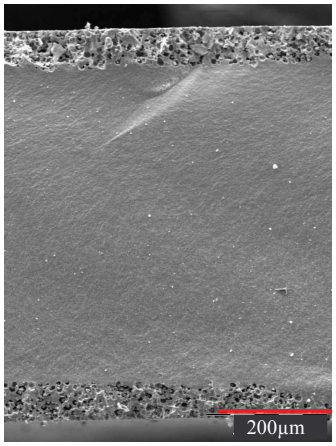

Fig.4. Cross section of the cathode/electrolyte/cathode cell (cathode porosity = 35.8%).

No delamination was observed at the interface of electrolyte and cathode materials. EDS analysis revealed no diffusion of the perovskite elements (Co, Mn) in the apatite structure (fig.5).

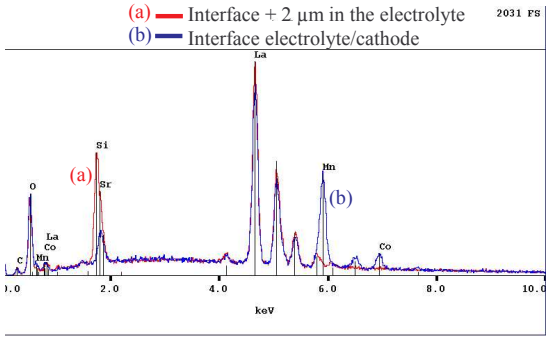

Fig.5. EDS analyses (a) in the apatite material at 2 µm from the interface and (b) at the interface of $La_9Sr_1(SiO_4)_6O_{2.5}$ apatite and $La_{0.75}Sr_{0.25}Mn_{0.8}Co_{0.2}O_{3-\delta}$ perovskite materials.

Impedance spectroscopy measurements were performed on the symmetrical cathode/electrolyte/cathode cells sintered at 1400°C-2h (fig. 6).

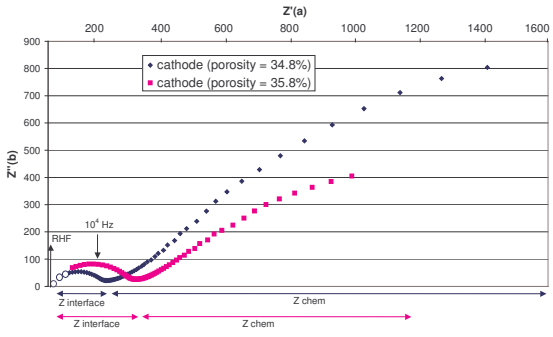

Fig.6. Nyquist diagram at 700°C of symmetrical cells $La_{0.75}Sr_{0.25}Mn_{0.8}Co_{0.2}O_{3-\delta}$/ $La_9Sr_1(SiO_4)_6O_{2.5}$/ $La_{0.75}Sr_{0.25}Mn_{0.8}Co_{0.2}O_{3-\delta}$ sintered at 1400°C-2h.

The kinetic of O_2 reduction on a mixed-conducting electrode has been treated by the Adler-Lane-Steele (ALS) model [14-16]. The impedance of a symmetrical cell can be expressed as:

$$Z = R_{electrolyte} + Z_{interfaces} + Z_{chem} \quad (1)$$

where $R_{electrolyte}$ is the electrolyte resistance, $Z_{interfaces}$ is the impedance of the electron-transfert and ion-transfert processes occurring at the current collector/electrode and electrolyte/electrode interfaces, respectively, and Z_{chem} includes oxygen surface exchange, solid-state diffusion of O^{2-} and gas-phase diffusion inside and outside the electrode.

Conductivity values, calculated from the resistance RHF, were respectively 4.6 10^{-3} and 4.7 10^{-3} S/cm at 700°C for the cathode containing respectively 34.8% and 35.8% of porosity. These values were close to $La_9Sr_1(SiO_4)_6O_{2.5}$ one (4.7 10^{-3} S/cm). RHF could be attributed to the ohmic loss of the electrolyte.

$Z_{interface}$ is higher for the cathode containing a porosity of 35.8%, which means that the charge transfer at the interface of electrolyte and cathode is more difficult when the cathode is more porous, though the difference of porosity is low, i.e. 1%. However, the electrode resistance (Z_{chem}) is lower, indicating a better gas-phase diffusion inside the more porous cathode material.

Some improvements have to be made on the cathode material in order to reduce the electrode and the charge transfer resistances:

- the cathode porosity should be increased in order to improve the rate of gas transport through the porous electrode and the absorption of O_2 molecules. A PFA volume fraction of 49.7% has been introduced in the tape casting suspension, leading to a porosity of 42.7% after sintering at 1400°C-2h.
- a composite cathode consisting of a mixture of perovskite and apatite materials should be elaborated in order to increase the triple phase boundary surface and so reducing the charge transfer resistance at the interface of electrolyte and cathode materials[17].

Conclusion

Electrochemical analyses have been performed on electrolyte and cathode materials as well as on symmetrical cathode/electrolyte/cathode cells. These materials were elaborated by tape casting and sintering at 1400°C-2h in air.

The presence of secondary phases could block the conduction of O^{2-} when the electrolyte is sintered at low temperature, i.e. 1400°C.

Concerning the co-sintered symmetrical cell, neither delamination nor reactivity between apatite and perovskite materials has been observed. However, the cathode material has to be improved in order to reduce the electrode and the charge transfer resistances.

References

1. S.Nakayama, M.Sakamoto, M.Higuchi, K.Kodaira, M.Sato, S.Kakita, Oxide ionic conductivity of apatite type $Nd_{9.33}(SiO_4)_6O_2$ single crystal, Journal of the European Ceramic Society, **19** (1999) 507
2. S.Nakayama, M.Sakamoto, M.Highchi, K.Kodaira, Ionic conductivities of apatite type NdX(SiO4)6O1.5X−12 (X□=□9.20 and 9.33) single crystals, Journal of Materials Science Letters, **19** (2000) 91
3. S.Nakayama, T. Kageyama, H.Aono, Y.Sadaoka, Ionic conductivity of lanthanoid silicates, $Ln_{10}(SiO_4)_6O_3$ (Ln = La, Nd, Sm, Gd, Dy, Y, Ho, Er and Yb), Journal of Materials Chemistry, **5** (1995) 1801
4. S.Nakayama and M.Higuchi, Electrical properties of apatite-type oxide ionic conductors $RE_{9.33}(SiO4)_6O_2$ (RE=Pr, Nd and Sm) single crystals, Journal of Materials Science Letters, **20** (2001) 913
5. E.J.Abram, D.C.Sinclair and A.R.West, A novel enhancement of ionic conductivity in the cation-deficient apatite $La_{9.33}(SiO_4)_6O_2$, Journal of Materials Chemistry, **11** (2001) 1978
6. L.Leon-Reina,, E.R.L.A.Cabeza, M.Martinez-Lara, S.Bruque, Journal of Materials Chemistry, **14** (2004) 1142
7. J.E.H.Sansom and P.R.Slater, Synthesis and structural characterisation of the apatite-type phases $La_{10-x}Si_6O_{26+z}$ doped with Ga, Solid State Ionics, **167** (2004) 17
8. J.E.H.Sansom, D.Richings and P.R.Slater, A powder neutron diffraction study of the oxide-ion-conducting apatite-type phases, $La_{9.33}Si_6O_{26}$ and $La_8Sr_2Si_6O_{26}$, Solid State Ionics, **139** (2001) 205
9. H.Arikawa, H.Nishiguchi, T.Ishihara. and Y.Takita, Oxide ion conductivity in Sr-doped $La_{10}Ge_6O_{27}$ apatite oxide, Solid State Ionics, **31** (2000) 136
10. A.Brisse, Thesis, September 2006
11. A.Vincent, S.Beaudet-Savignat, F.Gervais, Elaboration and ionic conduction of apatite-type lanthanum silicates doped with Ba, $La_{10-x}Ba_x(SiO_4)_6O_{3-x/2}$ with x = 0.25–2, Journal of the European Ceramic Society, **27** (2007) 1187
12. H.Ullmann, N.Trofimenko, F.Tiez, D.Stöver, A.Ahmad-Khanlou, Correlation between thermal expansion and oxide ion transport in mixed conducting perovskite-type oxides for SOFC cathodes, Solid State Ionics, 138 (2000) 79
13. Derek.J, *Zview*, I.Scrinner Associates, Editor 2005
14. S.B.Adler, J.A.Lane, B.C.H.Steele, Fundamental Issues in Modeling of Mixed-Conductors, Journal of the Electrochemical Society, **144 (5)** (1997) 1635
15. S.B.Adler, J.A.Lane, B.C.H.Steele, Fundamental Issues in Modeling of Mixed-Conductors, Journal of the Electrochemical Society, **144 (5)** (1997) 1884
16. S.B.Adler, Mechanism and kinetics of oxygen reduction on porous $La_{1-x}Sr_xCoO_{3-\delta}$ electrodeS, Solid State Ionics, **111 (1-2)** (1998) 125
17. V.Dusastre, J.A.Kilner, Optimisation of composite cathodes for intermediate temperature SOFC applications, Solid State Ionics, **126** (1999) 163